Published in final edited form as:
ACS Appl Mater Interfaces. 2012 June 27; 4(6): 2847–2854. doi:10.1021/am300467w.

Near-Infrared Emitting Squaraine Dyes with High 2PA Cross Sections for Multiphoton Fluorescence Imaging

Hyo-Yang Ahn[a], **Sheng Yao**[a], **Xuhua Wang**[a], and **Kevin D. Belfield**[a,b,*]

[a]Department of Chemistry, University of Central Florida, P.O. Box 162366, Orlando, FL 32816-2366, USA

[b]CREOL, The College of Optics and Photonics, University of Central Florida, P.O. Box 162366, Orlando, FL 32816-2366, USA

Abstract

Designed to achieve high two-photon absorptivity, new near infrared (NIR) emitting squaraine dyes, (E)-2-(1-(2-(2-methoxyethoxy)ethyl)-5-(3,4,5-trimethoxystyryl)-1H-pyrrol-2-yl)-4-(1-(2-(2-methoxyethoxy)ethyl)-5-(3,4,5-trimethoxystyryl)-2H-pyrrolium-2-ylidene)-3-oxocyclobut-1-enolate (**1**) and (Z)-2-(4-(dibutylamino)-2-hydroxyphenyl)-4-(4-(dibutyliminio)-2-hydroxycyclohexa-2,5-dienylidene)-3-oxocyclobut-1-enolate (**2**) were synthesized and characterized. Their linear photophysical properties were investigated via UV-visible absorption spectroscopy and fluorescence spectroscopy in various solvents, while their nonlinear photophysical properties were investigated using a combination of two-photon induced fluorescence and open aperture z-scan methods. Squaraine **1** exhibited a high two-photon absorption (2PA) cross section (δ_{2PA}), ~ 20,000 GM at 800 nm, and high photostability with the photochemical decomposition quantum yield one order of magnitude lower than Cy 5, a commercially available pentamethine cyanine NIR dye. The cytotoxicity of the squaraine dyes were evaluated in HCT 116 and COS 7 cell lines to assess the potential of these probes for biomedical imaging. The viability of both cell lines was maintained above 80% at dye concentrations up to 30 μM, indicating good biocompatibility of the probes. Finally, one-photon fluorescence microscopy (1PFM) and two-photon fluorescence microscopy (2PFM) imaging was accomplished after incubation of micelle-encapsulated squaraine probes with HCT 116 and COS 7 cells, demonstrating their potential in 2PFM bioimaging.

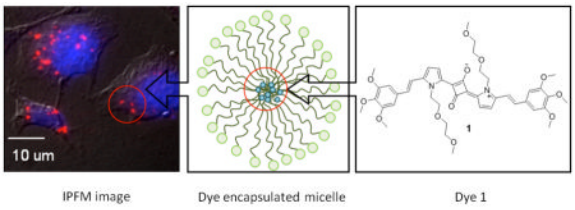

Belfield@ucf.edu.

Supporting Information Available.

^{1}H NMR and ^{13}C NMR are available in the Supporting Information for compounds **3** and **4** and SQ **1**, along with linear photophysical spectra and photodecomposition quantum determination yield data, thermostability analyses of SQ **1** and **2**, linear and nonlinear optical spectra of SQ **1**, SQ **2**, and **Cy5** in micelles, cytotoxicity of SQ **1** and **2**, and 1PFM images of SQ **1** and **2** in HCT 116 and COS 7 cell lines. This material is available free of charge via the internet at http://pubs.acs.org.

Keywords

Near infrared (NIR) dyes; squaraine; linear and nonlinear optical properties; bioimaging; two-photon fluorescence microscopy

Introduction

Squaraine dyes were initially developed and studied in the 1950's and 1960's.[1–3] There has been interest in squaraine compounds because of their unique properties that include a relatively narrow absorption band and emission in near-infrared (NIR) range. NIR emitting dyes have substantial potential for applications in photonics and biomedical fields such as photoconductivity,[4] solar energy conversion,[5–8] optical data storage,[9, 10] light emitting field-effect transistors,[11] nonlinear optics,[12] NIR-emitting fluorescent probes,[13] and sensitizers for photodynamic therapy.[14–17] In biophotonics research, NIR fluorescent dyes are desirable for noninvasive quantification and visualization via optical imaging in the window between 700 and 1000 nm range where a number of biological materials have high transparency. This wavelength region is critical in order to obtain deep penetration in tissue since most tissues have pronounced absorption below 700 nm. Additionally, photodamage and photobleaching may be reduced with NIR excitation.

For bioimaging, an ideal NIR probe needs to have high photochemical stability, low toxicity, high fluorescence quantum yield, and insensitivity to intermolecular quenching.[18] Conjugated cyanine dyes have been reported as NIR fluorescent dyes.[14, 19] However, the more π-conjugated a cyanine dye is, generally the less photostable it is.[20] On the other hand, squaraine dyes are generally promising as NIR fluorescent probes.[21] Johnson et al. reported that squaraine-rotaxane compound was well-demonstrated as stable NIR probe compared with Cy5 in terms of staining capabilities.[22] Two-photon absorption (2PA) is an important means of exciting a NIR fluorescent probe for noninvasive sensing and imaging in biological tissues.[1] Two-photon fluorescence microscopy (2PFM) imaging can provide better contrast, brighter images, and greater detail relative to conventional or one-photon fluorescence microscopy (1PFM).[16] In combination with 2PFM, a suitable squaraine-based probe may provide a unique toolset for three-dimensional (3D) bioimaging. Recently, a few cyanine dyes and squaraine (SQ) dyes were found to exhibit very high 2PA cross sections[24–26] while others were found to exhibit liquid crystalline properties.[27] However, the potential of SQ dyes as two-photon fluorescence probes has not been fully explored.

In this work, a new two-photon absorbing NIR squaraine dye, (E)-2-(1-(2-(2-methoxyethoxy)ethyl)-5-(3,4,5-trimethoxystyryl)-1H-pyrrol-2-yl)-4-(1-(2-(2-methoxyethoxy)ethyl)-5-(3,4,5-trimethoxystyryl)-2H-pyrrolium-2-ylidene)-3-oxocyclobut-1-enolate (**1**) was synthesized, characterized, and its application as a 2PFM probe was evaluated. In addition, (Z)-2-(4-(dibutylamino)-2-hydroxyphenyl)-4-(4-(dibutyliminio)-2-hydroxycyclohexa-2,5-dienylidene)-3-oxocyclobut-1-enolate (**2**), shown to possess a high 2PA cross section in our previous work[28] was also evaluated as a 2PFM probe. The commercially available pentamethine cyanine dye, **Cy5**, was studied for comparison. Most squaraine dyes are not soluble in water, a major obstacle for bioimaging, necessitating strategies to enhance their biocompatibility.[18] To address the solubility problem, amphiphilic copolymer was employed to facilitate micelle encapsulation[29] of SQ dyes **1** and **2**.

Experimental Materials and Methods

Synthesis

General—All reagents and solvents were used as received from commercial suppliers. Reactions were conducted under N_2 or Ar atmosphere. Melting points are uncorrected. ^1H and ^{13}C NMR spectra were recorded on a NMR spectrometer at 300 and 75 MHz, respectively. MS analyses were performed at the University of Florida. (Z)-2-(4-(Dibutylamino)-2-hydroxyphenyl)-4-(4-(dibutyliminio)-2-hydroxycyclohexa-2,5-dienylidene)-3-oxocyclobut-1-enolate (**2**) was prepared as reported previously.[21] **Cy5** (DiD oil, D 307) was obtained from Invitrogen (Carlsbad, CA)

1-(2-(2-Methoxyethoxy)ethyl)-1H-pyrrole-2-carbaldehyde 3: A mixture of 1*H*-pyrrole-2-carbaldehyde (0.476 g, 5.0 mmol), KOH (0.28 g, 5.0 mmol), and 18-crown-6 (0.04 g, 0.15 mmol) in C_6H_6 was refluxed for 2 h, then $BrCH_2CH_2OCH_2CH_2OCH_3$ (1.14 g, 6.25 mmol) in C_6H_6 was added and the mixture was refluxed for 4 h. Upon cooling, water was added and the organic phase was separated, washed with water and dried by $MgSO_4$. Concentration and purification by column chromatography using CH_2Cl_2/MeOH (100/1) as eluent gave 0.78 g product **3** as a liquid (yield 79%). ^1H NMR (300 MHz, $CDCl_3$) δ 9.49 (s, 1H), 7.04 (m, 1H), 6.91 (m, 1H), 6.18 (m, 1H), 4.48 (t, *J* = 6.0 Hz, 2H), 3.73 (t, *J* = 4.5 Hz, 2H), 3.46 (m, 2H), 3.42 (m, 2H), 3.31 (s, 3H). ^{13}C NMR (75 MHz, $CDCl_3$) δ 179.4, 132.8, 125.1, 110.0, 109.5, 71.8, 70.7, 70.5, 59.0, 48.8. HRMS (APCI) theoretical $[M+Na]^+$ = 220.0944, found $[M+Na]^+$ = 220.0941.

1-(2-(2-Methoxyethoxy)ethyl)-2-(3,4,5-trimethoxystyryl)-1H-pyrrole 4: 5-(Chloromethyl)-1, 2, 3-trimethoxybenzene (0.86 g, 4.0 mmol) was refluxed with triethyl phosphite (1.5 mL) for 2 h, the excess triethyl phosphite was distilled off and the residue was dried under vacuum. The product was then mixed with compound **3** in dry DMF (3 mL) under Ar. NaH (0.48 g, 20.0 mmol) was added and the mixture was stirred at room temperature for 20 h. The mixture was diluted with water and the product was extracted with ethyl acetate. Purified by column chromatography using ethyl acetate as eluent gave 0.7 g of product **4** (yield 48%) as a liquid. ^1H NMR (300 MHz, CDCl3) δ 6.91 (d, *J* = 9.0 Hz, 1H), 6.82 (d, *J* = 9.0 Hz, 1H), 6.75 (m, 1H), 6.68 (s, 2H), 6.48 (m, 1H), 6.18 (m, 1H), 4.20 (t, *J* = 4.5 Hz, 2H), 3.93 (s, 6H), 3.87 (s, 3H), 3.76 (*J* = 4.5 Hz, 2H), 3.56 (m, 2H), 3.51 (m, 2H), 3.36 (s, 3H). ^{13}C NMR (75 MHz, $CDCl_3$) δ 153.4, 137.5, 133.7, 131.6, 123.7, 123.1, 122.9, 108.8, 108.6, 106.7, 106.5, 103.1, 71.9, 71.1, 70.7, 61.0, 59.1, 56.3, 56.1, 46.7. HRMS (APCI) theoretical $[M+H]^+$ = 362.1962, found $[M+H]^+$ = 362.1971.

(E)-2-(1-(2-(2-Methoxyethoxy)ethyl)-5-(3,4,5-trimethoxystyryl)-1H-pyrrol-2-yl)-4-(1-(2-(2-methoxyethoxy)ethyl)-5-(3,4,5-trimethoxystyryl)-2H-pyrrolium-2-ylidene)-3-oxocyclobut-1-enolate (1): Compound **4** (0.70g, 2.00 mmol) and squaric acid (0.11 g, 0.97 mmol) in a BuOH/toluene mixture (2/1 v/v, 60 ml) were refluxed with a Dean-Stark apparatus for 6 h. The precipitated product was collected by filtration giving 0.31 g product **1**. (40% yield) m. p. 203–204 °C. ^1H NMR (300 MHz, $CDCl_3$) δ 7.84 (d, J = 3.0 Hz, 1H), 7.24 (d, J = 9.0 Hz, 1H), 7.16 (d, J = 9.0 Hz), 6.89 (d, J = 3.0 Hz, 1H), 6.77 (s, 4H), 4.96 (m, 4H), 3.94 (s, 12H), 3.89 (m, 6H+4H), 3.53 (m, 4H), 3.41 (m, 4H), 3.20 (s, 3H). ^{13}C NMR (75 MHz, $CDCl_3$) δ 177.0, 167.2, 153.5, 147.8, 139.2, 135.4, 134.9, 132.1, 129.9, 124.2, 116.2, 115.7, 113.9, 105.0, 104.3, 103.7, 72.08, 71.9, 70.7, 61.1, 58.8, 56.3, 56.2, 47.1. HRMS (ESI-TOF) theoretical $[M+Na]^+$ = 823.3412, found $[M+Na]^+$ = 823.3356.

Methods

Linear optical properties

Steady-state linear absorption was measured with an Agilent 8453 UV-vis spectrophotometer. Fluorescence emission and excitation spectra were measured using a PTI Quantamaster spectrofluorimeter equipped with a Hamamatsu R928 photomultiplier tube (PMT) in solvents of varying polarity. Fluorescence quantum yields were relative to cresyl violet as a reference.[30] Excitation anisotropy spectra were measured using a PTI Quantamaster spectrofluorimeter fitted with two Glan-Thomson polarizers in an L-format method in high viscosity solvent (glycerol, Acros) to avoid reorientation, and in low concentration solutions ($C \sim 10^{-6}$ M) to avoid reabsorption.[31]

Lifetime measurements were performed using a tunable Ti:sapphire laser system (Coherent Verdi-V10 and MIRA 900, pulse duration ~200 fs/pulse (FWHM), and repetition rate 76 MHz). The polarization of the excitation beam was linear (690 nm) and oriented by the magic angle to avoid molecular reorientation effects.[30] A broad band-pass filter (FF01-694/SP-25, Semrock) was placed in front of the avalanche photodiode detector (APD, PicoQuant GmbH, LSM_SPAD) allowing the collection of emission >700 nm. Data was acquired with a time-correlated single photon counting system (PicoHarp300).

The optical density of all the solutions did not exceed 0.12 at the excitation wavelength to avoid reabsorption. Measurements were conducted in 10 mm path length quartz cuvettes at room temperature. Linear photophysical properties of squaraines **1** and **2** were measured in acetonitrile (ACN), 1, 2-dichloromethane (DCM), dimethyl sulfoxide (DMSO), methanol (MeOH), tetrahydrofuran (THF), and Pluronic micelles that encapsulated the squaraine dye. All solvents were spectroscopic grade.

Nonlinear optical properties

The open aperture Z-scan method was performed using linear polarized excitation from a Clark-MXR, CPA2010, Ti:sapphire amplified system followed by an optical parametric generator/amplifier (model TOPAS 4/800, Light Conversion) providing laser pulses of 140 fs (FWHM) duration with 1 kHz repetition rate.[32] The tuning range was 520–2100 nm while $10^{-3}\text{M} \leq C \leq 10^{-2}\text{M}$ concentration solutions were used in a 1 mm quartz cuvette at room temperature between 780 and 860 nm. For the case of squaraine **1**, the same laser system coupled with a PTI Quantamaster Spectrofluorimeter was used for two-photon absorption (2PA) spectrum measurements of upconverted fluorescence under two-photon excitation over a broad spectral region from 840 to 1140 nm with $10^{-5}\text{M} \leq C \leq 10^{-3}\text{M}$ concentration DMSO solution in a 10 mm quartz cuvette at room temperature.[26] The 2PA spectrum of squaraine **1** was calibrated with ZnSe as a standard in the spectral region from 780 to 860 nm.[32]

Photochemical and thermal stability

Photochemical stability was evaluated for SQ **1**, SQ **2**, and **Cy5** in DMSO and aqueous micelle media by irradiating the solution in a 10 mm path length quartz cuvette using a 650 nm diode laser.[33–37] Time-dependent absorption spectra upon irradiation at 650 NM were obtained with an Agilent 8453 UV/Vis spectrophotometer and photodecomposition quantum yields were determined.

Thermostability was conducted by thermogravimetric analysis (TGA, Q 5000 TA Instruments) and differential scanning calorimetery (DSC, Q1000 TA Instruments).

Cell lines

HCT116 and COS 7 were purchased from America Type Culture Collection (ATCC, Manssas, VA, USA). All cells were incubated at 37 °C in a 95% humidified atmosphere containing 5% CO_2 in cell media (RPMI-1640, Invitrogen, Carlsbad, CA, USA), supplemented with 10% fetal bovine serum (FBS, Atlanta Biologicals, Lawrenceville, GA, USA), and 1% penicillin-streptomycin (Atlanta Biologicals, Lawrenceville, GA, USA). 0.25% Trypsin-EDTA (Invitrogen, Carlsbad, CA, USA) was used for cell splitting.

Micelle encapsulation

A concentrated micelle stock solution was prepared using 1 mg/mL of the dye by using a small amount of CH_2Cl_2 to dissolve the dye.[29] Water was added with 2 wt% of surfactant (Pluronic F 127 Prill, BASF Corporation) and stirred overnight. The crude solution was filtered before using. The concentration of the micelle-encapsulated probe stock solution was determined via UV-vis spectrophotometry using the molar absorptivity (SQ **1** $\varepsilon_{853} = 0.6 \times 10^5\ M^{-1}\ cm^{-1}$ and SQ **2** $\varepsilon_{601} = 1.0 \times 10^5\ M^{-1}\ cm^{-1}$).

Cytotoxicity assay

HCT116 and COS 7 were placed in 96 well plates 3×10^3 cells per well in 90 μL and incubated until there were 6×10^3 cells per well for the cytotoxicity assays.[38] The cells were incubated for additional 20 h with Pluronic micelle-encapsulated SQ dye in different concentrations. Subsequently, 10 μL of CellTiter 96® Aqueous One Solution reagent (MTS assay) was added into each well, followed by further incubation for 4 h at 37 °C. The relative viability of the cells incubated with SQ dyes to untreated cells was determined by measuring the MTS-formazan absorbance on a microplate reader (Spectra Max M5, Molecular Devices) at 490 nm with subtraction of the absorbance of the cell-free blank volume at 490 nm. The results from three individual experiments were averaged.

Cell culture and incubation

HCT116 and COS 7 cells were placed onto poly-D-lysine coated glass cover slips (12 mm, #1) in 24-well plates, 3×10^4 cells per well, and the cells were incubated for 48 h before incubating with the micelle-encapsulated dyes. The filtered stock solution was diluted with complete growth medium, RPMI-1640, and then incubated for 1.5 h. 20 μL of 5 μg/mL Hoechst nuclear stain was added followed by incubation for another 30 min. After incubation, the cells were washed with PBS (× 5) and fixed using 3.7% formaldehyde solution for 15 min at 37 °C. NaBH4 (1 mg/mL, prepared by adding a couple of drops of 0.1 M NaOH) solution in PBS (pH = 8.0) was added to each well (0.5 mL/well) for 15 min. The plates were then washed with PBS (× 2) and water (× 1). Finally, glass cover slips were mounted using Prolong Gold mounting media (Invitrogen) for microscopy.

One- and two-photon fluorescence microscopy (1PFM) and (2PFM) imaging

Conventional one-photon fluorescence images were obtained using an inverted microscope (Olympus IX70) equipped with a QImaging cooled CCD (Model Retiga EXi) and mercury lamp 100 W. In order to improve the fluorescence background-to-image ratios, customized filter cubes were used for the 1PFM images. The specifications of the filter cube were tailored to match the excitation wavelength of the probe, and to capture most of the probe's emission profile.

Two-photon fluorescence microscopy (2PFM) images were obtained with a modified Olympus Fluoview FV300 microscope system combined with a tunable Coherent Mira 900F Ti:sapphire laser, pumped by a 9 W Coherent Verdi 10 frequency doubled Nd:YAG laser. The femtosecond NIR laser beam (with ~200 fs pulse width and 76 MHz repetition rate) was

tuned to ~ 850 nm and used as the two-photon excitation source. Two-photon induced fluorescence was collected by a 60× microscopic objective (UPlanSApo 60×, NA = 1.35, Olympus). A high-transmittance broad short-pass filter (FF01-694/SP-25, Semrock) was placed in front of the PMT detector in the FV300 scanhead in order to filter out background radiation from the laser source.

Results and Discussion

SQ **1** was synthesized by condensation of squaric acid with pyrrole intermediate **4** in a 2:1 mixture of butanol and toluene using a Dean-Stark trap to azeotropely remove water (Scheme 1). Intermediate **4** was prepared by Horner-Emmons reaction of 1-(2-(2-methoxyethoxy)ethyl)-1H-pyrrole-2-carbaldehyde **3** with phosphonated 5-(chloromethyl)-1,2,3-trimethoxybenzene **2** in 48% yield. The dye structure was confirmed by ^{1}H NMR, ^{13}C NMR, and HRMS.

Linear photophysical properties of SQ dyes **1** and **2** are shown in Table 1. **Cy5** was characterized in DMSO and in Pluronic micelles for comparison purposes as a commercially available NIR dye. Both squaraines **1** and **2** had good solubility in most of the organic solvents used. The absorption and fluorescence emission spectra were characteristically narrow and sharp (see the spectra in the Supporting Information). Squaraine **1** exhibited absorption a maximum in the range from 688 to 706 nm and fluorescence emission maximum from 706 to 719 nm, depending on the solvent, while squaraine **2** has an absorption maximum in the range from 645 to 659 nm and fluorescence emission maximum from 657 to 675 nm, again depdending on solvent. Squaraine **1** showed about 50 nm longer absorption and fluorescence emission maxima than squaraine **2** and **Cy5**. The Stokes shift of the squaraines was relatively small, up to 18 nm, a common attribute of this class of molecules. Due to the poor water solubility of SQ **1** and **2**, they were encapsulated in micelles, and both exhibited a blue shift of about 50 nm from their original maximum peak as a result of specific intermolecular π-π interaction, i.e., *H*-aggregation.[39, 40]

All emission spectra were corrected by the spectral sensitivity of the PMT. Emission spectra were used for determination of the relative fluorescence quantum yield, Φ_{FL}, using the formula

$$\Phi_{FL} = \Phi_R \frac{I}{I_R} \frac{OD_R}{OD} \frac{n^2}{n^2_R} \frac{RP_R}{RP}$$

where the subscript *R* refers to the reference, Φ is the quantum yield, *OD* is the optical density, namely, absorption at the exciting wavelength, *n* is the refractive index of the solvent, *RP* is the relative power of the source beam of the fluorimeter at the excitation wavelength. Cresyl violet in methanol was used as a reference (Φ_{FL} = 0.54).[30] Φ_{FL} of SQ **1** and SQ **2** was a maximum 0.15 and 0.90 in an organic solvent, respectively (see Table 1). Φ_{FL} of the dyes in water soluble micelles decreased. Generally, fluorescence is significantly reduced in polar solvents such as water. In addition, when micelle-encapsulated dyes form aggregates, fluorescence quenching typically increases.[29, 41, 42] Generally, Φ_{FL} and fluorescence lifetime are strongly dependent upon each other and correlate well, consistent with our results.[43] Since squaraine **1** had a lower Φ_{FL}, it had correspondingly shorter lifetime between 0.16 and 0.51 ns, while the fluorescence lifetime of squaraine **2** was between 2.3 and 2.5 ns. Both probes exhibited a single exponential fluorescence decay process in the organic solvents studied.

Fluorescence anisotropy spectra were obtained by employing previously reported methods, using the equation:

$$r=\frac{I_{VV}-GI_{VH}}{I_{VV}+2GI_{VH}}, \quad (G=\frac{I_{HV}}{I_{HH}})$$

where G is a factor that is the ratio of the sensitivities of the detection system for vertically and horizontally polarized light.[30] The subscripts *V* and *H* refer to vertically and horizontally polarized light, respectively. Excitation anisotropy is different for different electronic transitions of a molecule, and is based on the angle between the absorption and emission dipole moments.[44] Anisotropy values can theoretically range from −0.2 to +0.4 due to the angles between transition dipole moments.[45] Hence, excitation anisotropy allows one to estimate energies (the spectral position) of various electronic transitions. These are useful to identify where one may expect to observe two-photon absorption since quantum mechanical selection rules are different for one- vs. two-photon absorption. SQ dye solutions were prepared in glycerol, a solvent with a high viscosity in order to avoid molecular reorientation. The dye was dissolved in methanol at high concentration and one drop was added into glycerol. The plateau above 560 nm in the anisotropy spectrum for SQ **1**, as shown in Figure 1, was associated with the low energy electronic transition ($S_0 \rightarrow S_1$) that is a one-photon allowed and, formally, a two-photon forbidden transition. The value of anisotropy decreased from 560 to 510 nm, suggesting a different electronic transition and increased until approximately 470 nm, creating a small valley. A similar trend was observed again from 440 to 350 nm. The specific valley regions, about 520 and 400 nm, respectively, suggest $S_0 \rightarrow S_n$ electronic transitions that are, potentially, two-photon allowed transitions. The analysis of the excitation anisotropy spectra and associated electronic transitions correlated well with the observed wavelength-dependent 2PA cross sections (Figure 1). The two minima in the anisotropy spectrum correspond to higher 2PA values than other wavelengths and the 2PA value at 800 nm was ~20,000 GM, approaching one of the highest values for squaraines reported.[28] Even at 1040 nm, a 2PA cross section of 1500 GM was recorded, indicating the potential use of this NIR probe in bioimaging since a large 2PA cross section is of considerable interest since the laser power to excite the molecule can be reduced, minimizing photodamage, an aspect that is particularly important for deep tissue penetration and live cell imaging.

SQ **2** was investigated and the 2PA cross section value was reported in one of our previous studies[28] (~13,000 GM at 730 nm in acetone). Since the 2PA cross sections of SQ **1** and **Cy5** were measured in DMSO, we measured the 2PA cross section of SQ **2** in DMSO as well for comparison. This measurement was performed by using a fs Ti:sapphire laser system (Coherent, Legend seeded by MIRA 900) that pumped an optical parametric amplifier (Coherent, OPerA Solo, FWHM ~ 100 fs, repetition rate = 1 kHz) using a PTI Quantamaster Spectrofluorimeter and a 10 mm quartz cuvette at room temperature. The tuning range was between 760 and 1030 nm for this specific measurement, with concentration in the range of $10^{-5}\text{M} \leq \text{C} \leq 10^{-3}$ M. Rhodamine B was used as a reference.

Excitation anisotropy and 2PA cross section values for SQ **2** are shown in Figure 2. Even though the highest value of the 2PA cross section did not exactly coincide with the anisotropy minimum, it was close (400 to 600 nm), indicating possible higher $S_0 \rightarrow S_n$ electronic transitions. The highest value of the 2PA cross section for SQ **2** was ~6000 GM at 860 nm, over two orders of magnitude higher than the commercially available **Cy5** (~500 GM at 820 nm, see Supporting Information).

2PA cross sections of the squaraine dyes were also measured in aqueous micelle media. SQ **1** exhibited a 2PA cross section up to ~3500 GM while the 2PA cross section of SQ **2** was up to ~2,000 GM. The 2PA of **Cy5** was ~100 GM under these conditions. The data indicate the nonlinear absorption of the compounds decreased upon micelle-encapsulation in aqueous media, yet SQs **1** and **2** exhibited two-photon absorptivity up to 35 times greater than the commercially available NIR dye **Cy5**.

Photostability is an important attribute for the application of probes in fluorescence microscopy due to prolonged or repeated irradiation of the compound.[46] The photochemical stability of the dyes was investigated in DMSO (see Supporting Information) and in aqueous micelle media to obtain a deeper insight into the relationship between the structure and photostability of the squaraine dyes. Commercial **Cy5** dye was studied for comparison. Measurements were obtained by irradiating the sample in a 10 mm path length quartz cuvette using a 650 nm diode laser (60 mW) and recording the differences between absorbance as a function of time as shown in Figure 3. The results indicated that the SQs **1** and **2** were more photostable than commercial **Cy5** in aqueous micelles. Photostability is defined by time-dependent variation in absorption maxima (A/A_0) of three dyes in Figure 3(d), a parameter that can be quantified by calculating the photochemical decomposition quantum yield (η).[26–30]

The results shown in Table 2 are averages of seven to ten pairs of adjacent maximum absorption values. SQ **1** was twice as stable than **Cy5** in DMSO while the photostability of the squaraine dyes was one order of magnitude higher than **Cy5** in aqueous micelle media.

The two-photon action cross section is means for estimating the relative efficiency of a fluorescence probe.[47] The two-photon action cross section is the product of the fluorescence quantum yield and the 2PA cross section (the highest value of 2PA spectrum of each dye), i.e., $\Phi_{FL}\cdot\delta_{2PA}$. The results indicate that the two-photon action cross section of our squaraine dyes is two orders of magnitude greater than **Cy5**. However, this value does not account for photostability. Thus, given the value of (photochemical decomposition quantum yield), a figure of merit (F_M) can be defined for a dye.[38] This is a measure of not only the efficiency of the probe but also its photostability, and can be derived from the two-photon action cross section normalized by η, i.e., $F_M = \Phi_{FL}\cdot\delta_{2PA}/\eta$.

Molar absorptivity, $\varepsilon(M^{-1}\cdot cm^{-1})$ fluorescence quantum yield, Φ_{FL}, maximum 2PA cross section, δ_{2PA}, photochemical decomposition quantum yield, η, two-photon action cross section, $\Phi_{FL}\cdot\delta_{2PA}$, and figure of merit, F_M.

In addition to photostability, thermal stability is also a key attribute of a compound, because even though temperatures that a probe may be exposed to are not typically very high, it will often be heated, e.g., in an incubator. Thermostability testing of squaraine dyes were performed using thermogravimetic analysis (TGA) and differential scanning calorimetry (DSC) (see Supporting Information). The thermal decomposition temperature, T_d, was determined by using TGA from the measurement of the change in mass of the sample with varying temperature. Thermostability can be determined by DSC, which measures the heat flow in the sample as a function of temperature. The T_d of SQ **1** was ca. 400 °C, exhibiting very high thermostability and stability through multiple heating and cooling scanning cycles. The T_d of SQ **2** was ca. 230 °C. The data indicated that both dyes have ample thermostability properties required for biological research.

Since we are considering squaraines **1** and **2** for potential bioimaging applications, biocompatibility is very important, yet little has been reported for squaraine dyes.[22] Cytotoxicity assays were performed using HCT 116 and COS 7 cell lines, two commonly

employed cell lines (see Supporting Information). HCT 116 is one of the human colorectal cancer cells. COS 7 is a kidney cell line from African green monkeys modified with SV40 virus. The concentrations of SQ **1** ranged from 0.1 to 20.0 μM, and, after 20 h incubation, the percent of viable cells remained above 80%. Likewise, the cell viability of SQ **2** was above 80% until 30 μM.

Based on the cell viability test results, all concentrations of 20 and 50 μM were employed for 1PFM and 2PFM imaging with SQ **1** in HCT 116 and COS 7 cells while concentration of 20 μM was selected for SQ **2** (shown in the Supporting Information). Customized filter cubes, fluo out (Ex 377/50, DM 409, Em 525/40) and Cy5 filter (Ex 630/50, DM 660, Em 690/40), were used for Hoechst (to visualize cell nuclei) and the SQ dye channels, respectively. Even though HCT 116 and COS 7 cell lines are quite different, our analysis shows that the probes appear to be uptaken similarly, likely into endosomes.

2PFM images were obtained using a fs Ti:sapphire Mira 900 laser tuned to 850 nm (70 mW, 694 nm short pass cutoff filter) as shown in Figure 4. Since the F_M value of both dyes is very high, the 2PFM images were very bright, suggesting the potential of these squaraine dyes for other bioimaging applications such as *ex vivo* and *in vivo* imaging, subjects of future investigations.

Conclusions

We report the linear and nonlinear photophysical properties of squaraine dyes **1** and **2** in several organic solvents and aqueous media via micelle-encapsulation. The relative quantum yields of both probes were reasonable and, not surprisingly, both exhibited somewhat reduced fluorescence quantum yields in aqueous micelle media. SQ **1** exhibited an impressive 2PA cross section of ca. 20,000 GM at 800 nm and ca. 1,000 GM at wavelengths just over 1,000 nm, creating several possibilities for two-photon based imaging at a variety of excitation wavelengths. The photostability of the SQ dyes was compared with commercially available NIR dye **Cy5**. The photostability of the new squaraine probes were one order of magnitude higher than **Cy5**, a significant finding in the development of probes for bioimaging, as photobleaching is too often a liability of NIR probes. The squaraine dyes were rather benign to HCT 116 and COS 7 cell lines with cell viability percent of at least ca. 80% even at dye concentrations up to 50 μM, an indication of good biocompatibility. One-photon fluorescence microscopy (1PFM) and two-photon fluorescence microscopy (2PFM) imaging was demonstrated for SQ probes **1** and **2** in both cell lines, proving high contrast images. These results suggest the potential utility of the probes for both conventional and two-photon fluorescence-based *ex vivo* and *in vivo* bioimaging.

Supplementary Material

Refer to Web version on PubMed Central for supplementary material.

Acknowledgments

We wish to acknowledge the National Institute of Biomedical Imaging and Bioengineering of the National Institutes of Health (1 R15 EB008858-01), the National Science Foundation (CHE-0832622 and CHE-0840431), and the National Academy of Sciences (PGA-P210877) for partial support of this work. We also acknowledge Dr. Lazaro A. Padilha for assistance with open aperture Z scan measurements.

References

1. Beverina L, Salice P. Eur J Org Chem. 2010; 7:1207–1225.
2. Treibs A, Jacob K. Angew Chem. 1965; 77:680–681.

3. Sprenger HE, Ziegenbein W. Angew Chem. 1966; 78:937–938.
4. Law K-Y. J Phys Chem. 1988; 92:4226–4231.
5. Yum J-H, Walter P, Huber S, Rentsch D, Geiger T, Nu F, Angelis FD, Gra M, Nazeeruddin MK. Langmuir. 2007; 129:10320–10321.
6. Wei G, Xiao X, Wang S, Zimmerman JD, Sun K, Diev VV, Thompson ME, Forrest SR. Nano Lett. 2011; 11:4261–4264. [PubMed: 21923102]
7. Bagnis D, Beverina L, Huang H, Silvestri F, Yao Y, Yan H, Pagani GA, Marks TJ, Facchetti A. J Am Chem Soc. 2010; 132:4074–4075. [PubMed: 20205468]
8. Bürckstümmer H, Tulyakova EV, Deppisch M, Lenze MR, Kronenberg NM, Gsänger M, Stolte M, Meerholz K, Würthner F. Angew Chem Int Ed. 2011
9. Corredor CC, Huang Z-L, Belfield KD. Adv Mater. 2006; 18:2910–2914.
10. Corredor CC, Huang Z-L, Belfield KD, Morales AR, Bondar MV. Chem Mater. 2007; 19:5165–5173.
11. Smits EB, Setayesh S, Anthopoulos TD, Buechel M, Nijssen W, Coehoorn R, Blom PWM, de Boer B, de Leeuw DM. Adv Mater. 2007; 19:734–8.
12. Chen C-T, Marder SR, Cheng L-T. J Am Chem Soc. 1994; 116:3117–3118.
13. Song B, Zhang Q, Ma W-H, Peng X-J, Fu X-M, Wang B-S. Dyes Pigm. 2009; 82:396–400.
14. Santos PF, Reis LV, Almeida P, Serrano JP, Oliveira AS, Ferreira LFV. J Photochem Photobiol A Photochem. 2004; 163:267–269.
15. Gayathri Devi D, Cibin TR, Ramaiah D, Abraham A. J Photochem Photobiol B, Biol. 2008; 92:153–159.
16. Ramaiah D, Eckert I, Arun KT, Weidenfeller L, Epe B. Photochem Photobiol. 2004; 79:99–104. [PubMed: 14974721]
17. Rapozzi V, Beverina L, Salice P, Pagani GA, Camerin M, Xodo LEJ. Med Chem. 2010; 53:2188–2196.
18. Arunkumar E, Fu N, Smith BD. Chem Eur J. 2006; 12:4684–4690. [PubMed: 16575935]
19. Kopainsky B, Qiu P, Kaiser W. Appl Phys B: Lasers Opt. 1982; 29:15–18.
20. Pham W, Lai W-F, Weissleder R, Tung C-H. Bioconjugate Chem. 2003; 14:1048–51.
21. Patonay G, Salon J, Sowell J, Strekowski L. Molecules. 2004; 9:40–9. [PubMed: 18007410]
22. Johnson JR, Fu N, Arunkumar E, Leevy WM, Gammon ST, Piwnica-Worms D, Smith BD. Angew Chem Int Ed. 2007; 46:5528–5531.
23. Schafer KJ, Belfield KD, Yao S, Frederiksen PK, Hales JM, Kolattukudy PE. J Biomed Opt. 2005; 10(5):051402-1–051402-8. [PubMed: 16292939]
24. Chung S-J, Zheng S, Odani T, Beverina L, Fu J, Padilha LA, Biesso A, Hales JM, Zhan X, Schmidt K, Ye A, Zojer E, Barlow S, Hagan DJ, Van Stryland EW, Yi Y, Shuai Z, Pagani GA, Bredas J-L, Perry JW, Marder SR. J Am Chem Soc. 2006; 128:14444–5. [PubMed: 17090012]
25. Odom SA, Webster S, Padilha LA, Peceli D, Hu H, Nootz G, Chung S-J, Ohira S, Matichak JD, Przhonska OV, Kachkovski AD, Barlow S, Bredas J-L, Anderson HL, Hagan DJ, Van Stryland EW, Marder SR. J Am Chem Soc. 2009; 131:7510–7511. [PubMed: 19435343]
26. Hu H, Gerasov AO, Padilha LA, Przhonska OV, Webster S, Shandura MP, Kovtun YP, Masunov AE, Hagan DJ, Stryland EWV. IEEE CLEO. 2010
27. Qaddoura MA, Belfield KD, Tongwa P, DeSanto JE, Timofeeva TV, Heiney PA. Supramol Chem. 2011; 23:731–742.
28. Toro C, De Boni L, Yao S, Ritchie JP, Masunov AE, Belfield KD, Hernandez FE. J Chem Phys. 2009; 130:1–6.
29. Andrade CD, Yanez CO, Qaddoura MA, Wang X, Arnett CL, Coombs SA, Yu J, Bassiouni R, Bondar MV, Belfield KD. J Fluoresc. 2011; 21:1223–1230. [PubMed: 21243414]
30. Lakowicz, JR. Principles of Fluorescence Spectroscopy. Springer; New York, NY: 2006.
31. Belfield KD, Bondar MV, Hales JM, Morales AR, Przhonska OV, Schafer KJ. J Fluoresc. 2005; 15:3–11. [PubMed: 15711871]
32. Sheik-bahae M, Said AA, Wei T-H, Hagan DJ, Van Stryland EW. IEEE J Quantum Electron. 1990; 26:760–769.

33. Belfield KD, Bondar MV, Morales AR, Padhila LA, Przhonska OV, Wang X. ChemPhysChem. 2011; 12:2755–2762. [PubMed: 21858908]
34. Corredor CC, Belfield KD, Bondar MV, Przhonska OV, Yao S. J Photochem Photobiol A Photochem. 2006; 184:105–112.
35. Belfield KD, Bondar MV, Przhonska OV, Schafer KJ. J Photochem Photobiol A Photochem. 2004; 162:489–496.
36. Belfield KD, Bondar MV, Przhonska OV, Schafer KJ. J Photochem Photobiol A Photochem. 2004; 162:569–574.
37. Belfield KD, Bondar MV, Przhonska OV, Schafer KJ. Photochem Photobiol Sci. 2004; 3:138–141. [PubMed: 14768631]
38. Wang X, Nguyen DM, Yanez CO, Rodriguez L, Ahn H-Y, Bondar MV, Belfield KD. J Am Chem Soc. 2010; 132:12237–12239. [PubMed: 20712313]
39. Tristani-Kendra M, Eckhardt CJ. J Chem Phys. 1984; 81:1160–1173.
40. Chen H, Farahat MS, Law K-y, Whitten DG. J Am Chem Soc. 1996; 118:2584–2594.
41. Tatikolov AS, Panova IG, Ishchenko AA, Kudinova MA. Biophysics. 2010; 55:35–40.
42. Muino PL, Callis PR. J Phys Chem B. 2009; 113:2572–7. [PubMed: 18672928]
43. Belfield KD, Bondar MV, Przhonska OV, Schafer KJ. J Fluoresc. 2002; 12:449–454.
44. Scheblykin IG, Drobizhev MA, Varnavsky OP, Vitukhnovsky MAG. Chem Phys Lett. 1996; 261:181–190.
45. Belfield KD, Bondar MV, Hernandez FE, Przhonskac OV, Yao S. Chem Physics. 2006; 320:118–124.
46. Song F. J Photochem Photobiol A Photochem. 2004; 168:53–57.
47. Mulligan SJ, Macvicar BA. Mod Res Edu Topics Microsc. 2007:881–889.

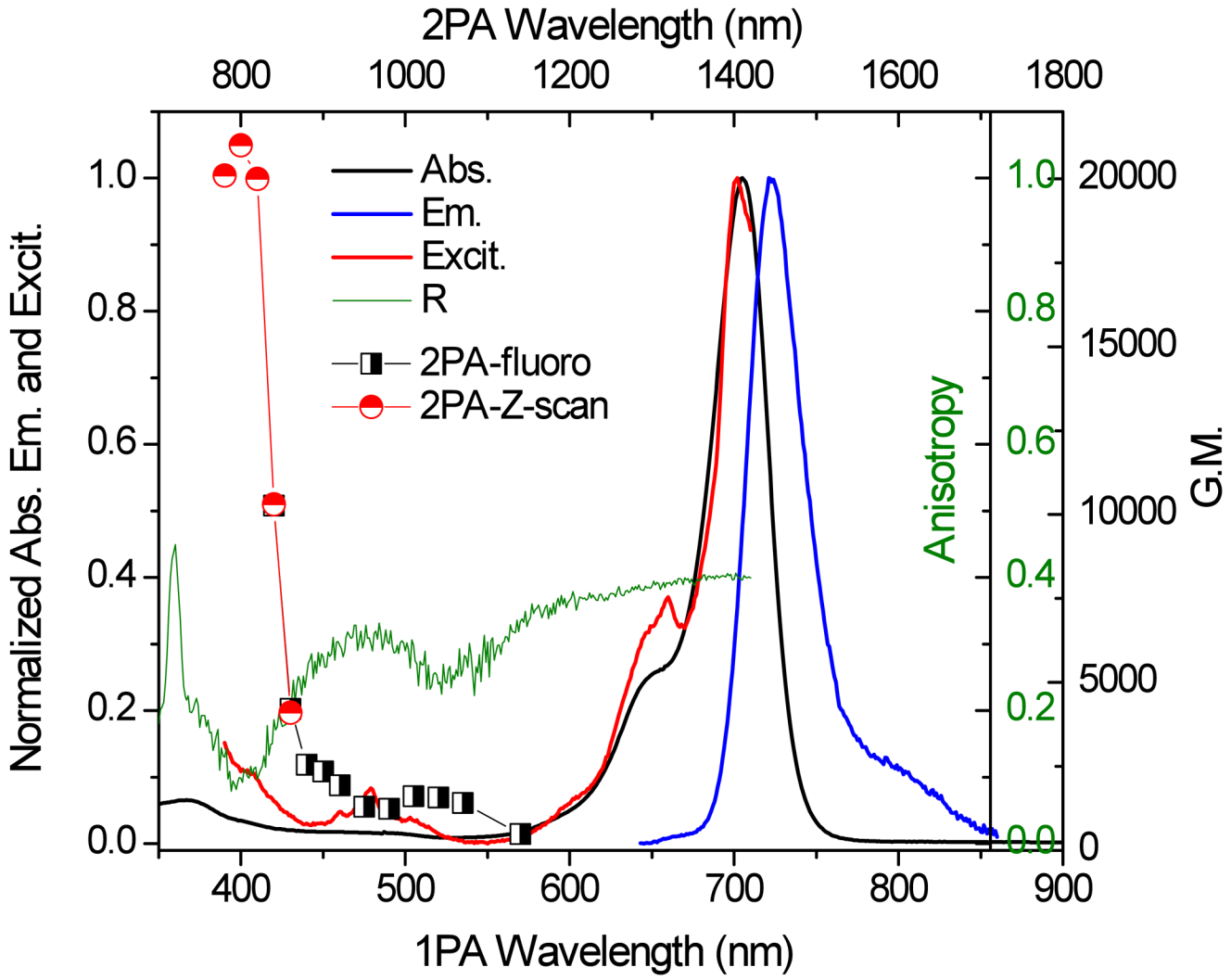

Figure 1.

Linear and nonlinear photophysical characterization of SQ **1** in DMSO (1 GM (Göppert Meyer) = 10^{-50} cm^4 s/photon^{-1}, uncertainty of the 2PA value = 15 %). Linear absorption (black), emission (blue), excitation (red), excitation anisotropy (green), and 2PA cross sections (two-photon fluorescence, black squares, and Z-scan, red circles).

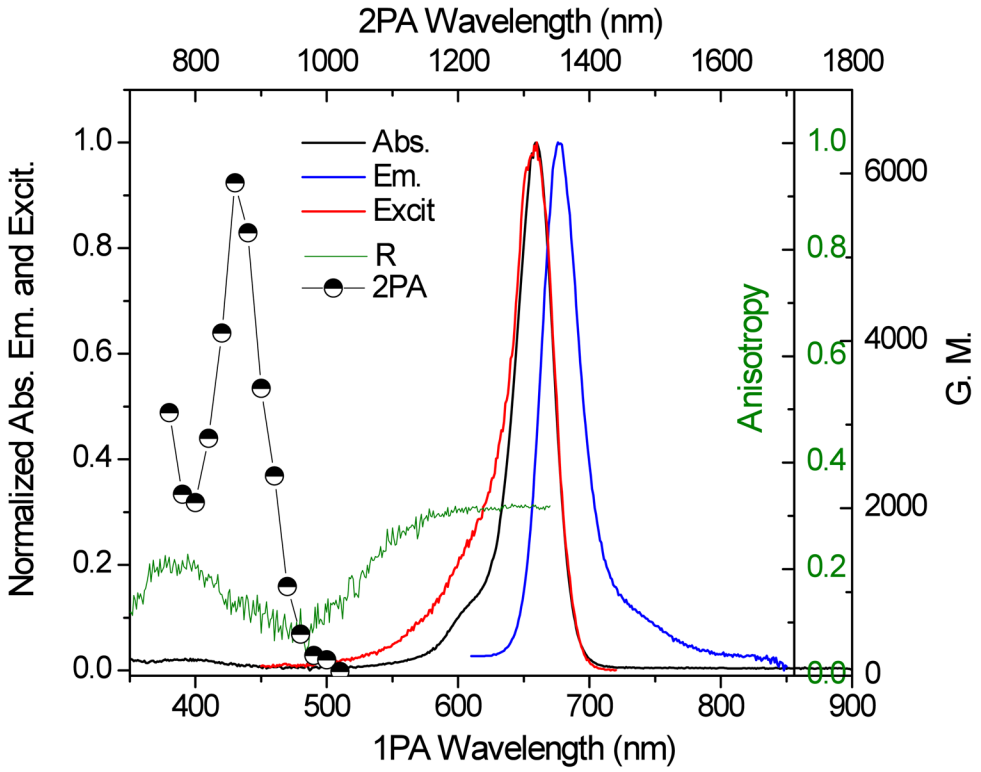

Figure 2.

Linear and nonlinear photophysical characterization of SQ **2** in DMSO (1 GM (Göppert Meyer) = 10^{-50} cm^4 s/photon^{-1}, uncertainty of the 2PA value = 15 %). Linear absorption (black), emission (blue), excitation (red), excitation anisotropy (green), and 2PA cross sections (Z-scan, black circles).

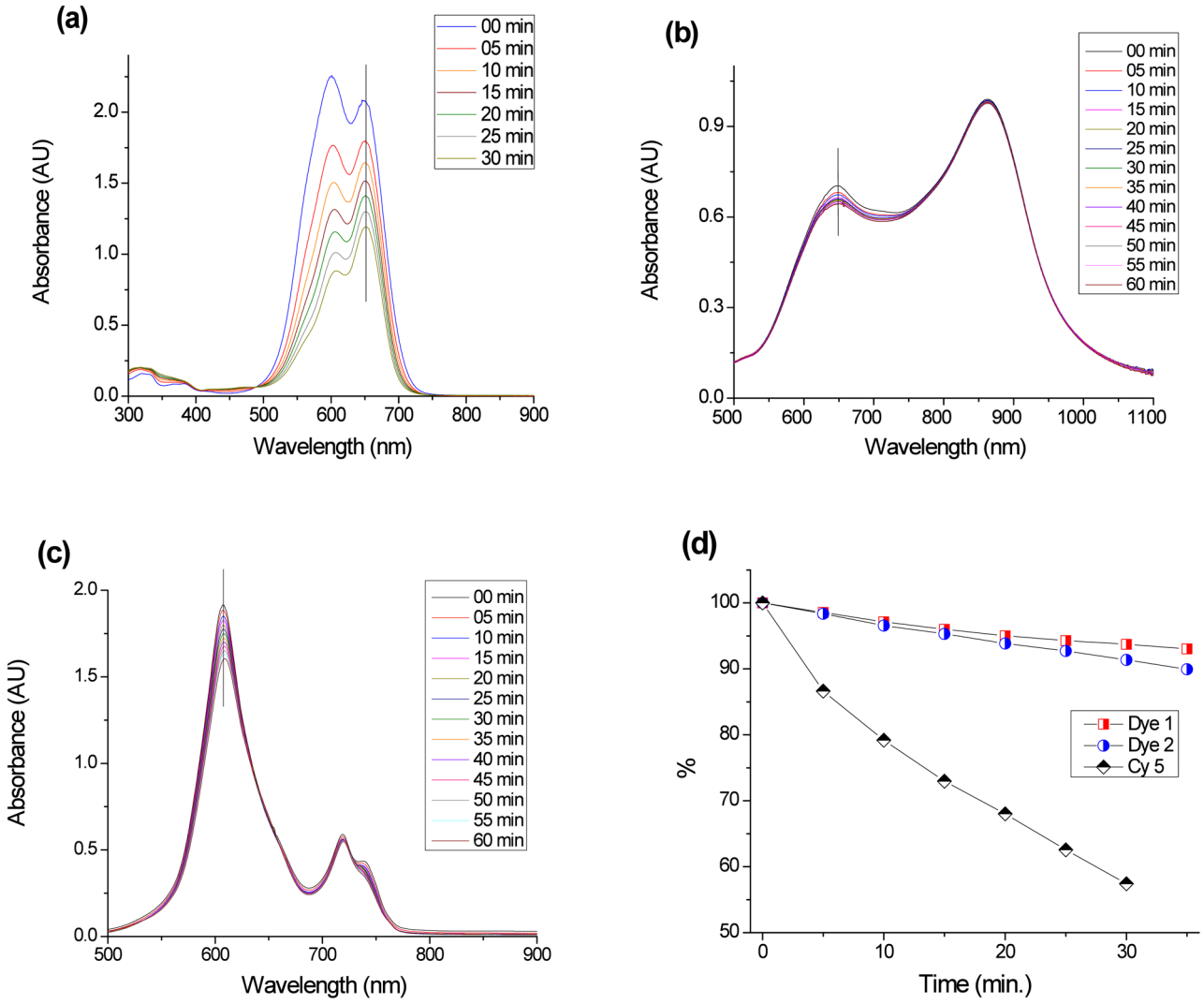

Figure 3.

Kinetic changes in the absorption spectra of the corresponding dyes excited at 650 nm in Ar-degassed micelles (a) **Cy5**, (b) SQ **1**, (c) SQ **2**, and (d) a plot of the percentage of the absorption at the wavelengths indicated by the vertical line in (a), (b), and (c) as a function of time for the three dyes.

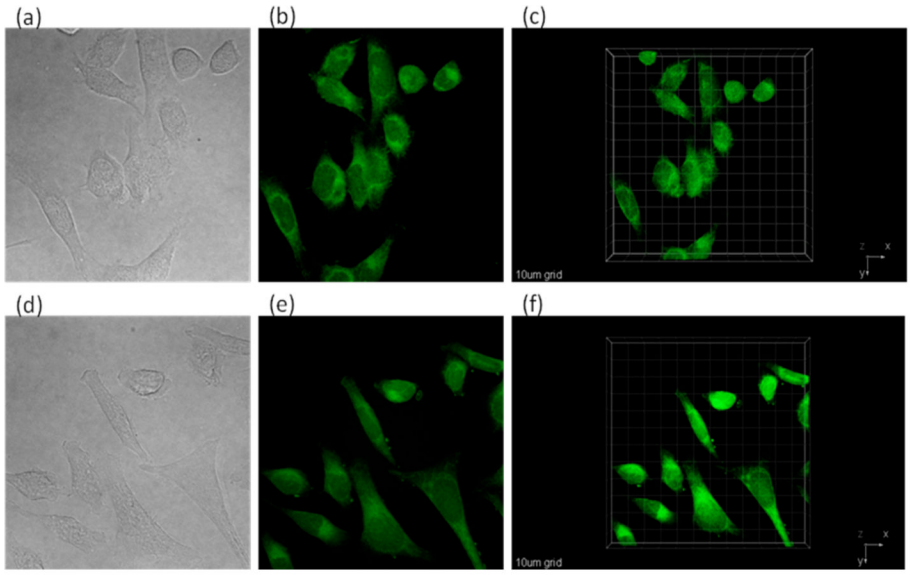

Figure 4.
Images of HCT 116 incubated with SQ **1** (a) DIC, (b) 2PFM (2D single X-Y optical section), and (c) 2PFM 3D reconstruction. Images of HCT 116 incubated with SQ **2** (d) DIC, (e) 2PFM (2D single X-Y optical section), and (f) 2PFM 3D reconstruction (scale bar = 10 μm).

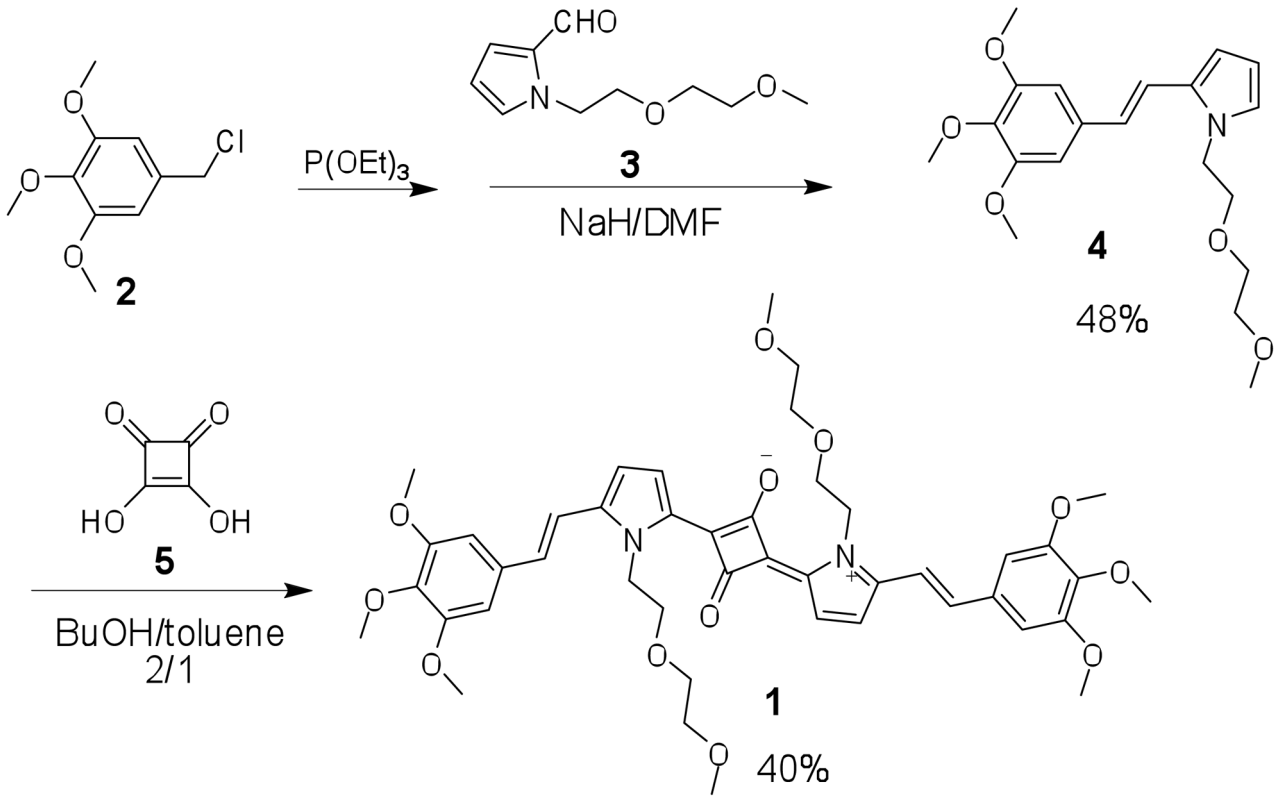

Scheme 1.

Table 1

Linear photophysical property data for dyes **1**, **2**, and **Cy5** in different solvents.

Dye	Solvent		Polarity	$\lambda^{Abs.}_{max}$	$\lambda^{Em.}_{max}$	Stokes Shift	Φ_{FL}	τ_{FL} (ns)	χ^2
Dye **1**	Aprotic	DCM	1.6	696 ± 1	711 ± 1	15 ± 2	0.07 ± 0.05	0.37 ± 0.07	0.99
		THF	1.75	699 ± 1	713 ± 1	14 ± 2	0.15 ± 0.03	0.53 ± 0.07	0.99
		ACN	3.92	688 ± 1	705 ± 1	17 ± 2	0.05 ± 0.01	0.24 ± 0.07	0.99
		DMSO	3.96	706 ± 1	719 ± 1	13 ± 2	0.11 ± 0.03	0.51 ± 0.07	0.99
	Protic	MeOH	1.7	688 ± 1	706 ± 1	18 ± 2	0.03 ± 0.02	0.16 ± 0.07	0.99
		Micelle	Water 1.85	647 ± 1	656 ± 1	9 ± 2	0.005 ± 0.001	1.8 ± 0.1	0.97
Dye **2**	Aprotic	DCM	1.6	648 ± 1	657 ± 1	9 ± 2	0.75 ± 0.05	2.4 ± 0.1	0.99
		THF	1.75	647 ± 1	657 ± 1	10 ± 2	0.80 ± 0.05	2.4 ± 0.1	0.98
		ACN	3.92	645 ± 1	660 ± 1	15 ± 2	0.75 ± 0.05	2.5 ± 0.1	0.99
		DMSO	3.96	659 ± 1	675 ± 1	16 ±1	0.62 ± 0.05	2.3 ± 0.1	0.99
	Protic	MeOH	1.7	644 ± 1	658 ± 1	14 ± 2	0.90 ± 0.05	2.3 ± 0.1	0.98
		Micelle	Water 1.85	606 ± 1	746 ± 1	40 ± 2	0.004 ± 0.001	2.7 ± 0.1	0.96
Cy 5	Aprotic	DMSO	3.96	651 ± 1	670 ± 1	19 ± 2	0.45 ± 0.05	1.7 ± 0.1	0.99
	Protic	Micelle	Water 1.85	650 ± 1	669 ± 1	19 ± 2	0.017 ± 0.005	2.2 ± 0.1 0.61 ± 0.07	0.99

Maxima of absorption, λ^{Abs}_{max} and fluorescence, λ^{Em}_{max}, fluorescence quantum yield, Φ_{FL}, lifetimes, τ, and correlation coefficient, χ^3.

Table 2

Photochemical decomposition quantum yields (η) and figure of merits (F_M) of SQ **1**, SQ **2**, and **Cy5** in DMSO and aqueous micelles.

Solvent	Dye	ε	Φ_{FL}	δ_{2PA}	η	$\Phi_{FL}\delta_{2PA}$	F_M
DMSO	SQ **1**	3.10E+05	0.11	20000	1.84E−06	2200	1.20E+09
	SQ **2**	2.90E+05	0.62	6000	2.74E−05	3720	1.36E+08
	Cy5	4.00E+05	0.45	500	2.37E−06	225	9.49E+07
Micelle	SQ **1**	5.50E+04	0.005	3500	4.60E−05	17.5	3.80E+05
	SQ **2**	1.00E+05	0.004	2000	6.50E−05	8	1.23E+05
	Cy5	1.50E+05	0.017	100	4.38E−04	1.7	3.88E+03